RSC Advances

ROYAL SOCIETY OF CHEMISTRY

www.rsc.org/advances

Abnormal dielectric properties and phase transition in $Bi_{0.783}(Mo_{0.65}V_{0.35})O_4$ scheelite-related structured ceramic

Di Zhou,[*a,b] Wen-Bo Li,[a] Li-Xia Pang,[c] Zhen-Xing Yue,[d] Guang-Sheng Pang[e] and Xi Yao[a]

[a]Electronic Materials Research Laboratory, Key Laboratory of the Ministry of Education & International Center for Dielectric Research, Xi'an Jiaotong University, Xi'an 710049, Shaanxi, China

[b]Xi'an Jiaotong University Suzhou Academy, Suzhou 215123, Jiangsu, China

[c]Micro-optoelectronic Systems Laboratories, Xi'an Technological University, Xi'an 710032, Shaanxi, China

[d]State Key Laboratory of New Ceramics and Fine Processing, Department of Materials Science and Engineering, Tsinghua University, Beijing 100084, PR Chin

[e]State Key Laboratory of Inorganic Synthesis and Preparative Chemistry, Jilin University, Changchun 130021, Jilin, China

[*]Corresponding author. Tel: +86-29-82668679; Fax: +86-29-82668794; E-mail address: zhoudi1220@gmail.com (Di Zhou),

Abstract

In the present work, an interesting phase transition at 150 $^{\circ}$C in ordered scheelite structured $Bi_{0.783}(Mo_{0.65}V_{0.35})O_4$ ceramic was observed for the first time. This phase transition was believed to be related to the ordered arrangement of A site defect (or A site cations Bi^{3+}). X-ray diffraction (XRD) and Raman spectra were employed to study the structure. Thermal expansion data showed that a sudden decrease in cell volume was observed during the phase transition, which resulted in the sharp increase in dielectric permittivity and loss over a wide frequency range (100 Hz ~ 7.5 GHz). Far-infrared reflectivity and THz spectra were used to study the intrinsic dielectric properties. It was found that the Bi-O stretches contributed mainly to the polarization. This study extended the design of A site ordered scheelite structured materials and the knowledge of their phase transitions.

I. Introduction

The scheelite structure (general formula ABO_4, in which A is 8-coordinated and B is 4-coordinated) has been studied for decades, due to their catalytic and dielectric properties.[1,2] Among the scheelite structured materials, $BiVO_4$ material has attracted more and more attention recently, due to its application in visible light water-splitting as a photocatalysis and microwave dielectrics as a high-K material.[1-4]

$BiVO_4$ possesses four different structures and the monoclinic scheelite structured $BiVO_4$ is recognized as the most useful one, in which the VO_4 tetrahedra is slightly distorted (with one long V-O bond and one short V-O bond).[3-5] It has been found that large concentration of defects could occur at A site of the scheelite structure. The defect composition could be written as $A_{1-x}\Phi_x MoO_4$, where the Φ represents defect.[1] The largest content of defect of 1/3 could be formed in high temperature quenched $La_{2/3}\Phi_{1/3}MoO_4$. Usually the cation vacancies (or cations at A site) took on an ordered arrangement, such as those in $Eu_2(WO_4)_3$, $Bi_2(MoO_4)_3$, $Nd_2(MoO_4)_3$ etc,[6-8] along with the distortion of BO_4 tetrahedra. These interesting modifications offer an opportunity to design some novel scheelite structured-related solid solutions.

In our previous work, phase composition and microwave dielectric properties of $xBi_{2/3}MoO_4$–$(1 - x)BiVO_4$ $(0.0 \leq x \leq 1.0)$ ceramics were studied in detail.[9] It was found that a novel ordered scheelite phase region was formed in the range $0.5 \leq x < 0.7$, in which a series of super-lattice X-ray diffraction (XRD) peaks was observed. In the present work, in-situ XRD, Raman spectra, thermal expansion curve, dielectric spectroscopy and infrared reflectivity (including THz spectra) were employed to study the crystal structure and phase transition in the typical ordered scheelited $xBi_{2/3}MoO_4$–$(1 - x)BiVO_4$ (x = 0.65, abbreviated as $Bi_{0.783}(Mo_{0.65}V_{0.35})O_4$.

II. Experimental Methods

The $xBi_{2/3}MoO_4$-(1-x)$BiVO_4$ (0.0 ≤ x ≤ 1.0) ceramics were prepared by using the solid state reaction method as described in our previous work.[9] High temperature XRD was performed from room temperature to 380 °C by using a XRD with Cu Ka radiation (X'Pert PRO, PANalytical, Holland). Prior to examination, sintered pellets were crushed in a mortar and pestle to powder. The diffraction pattern was obtained between 10 ~ 65 ° (2θ) at a step size of 0.02 °. Thermal expansion parameters were measured by using a dilatometer (DIL402C, NETZSCH, Germany). Differential Thermal Analysis (DTA) was carried out by using a thermoanalyzer system (Netzsch STA-449C, Netzsch, Selb, Germany) with heating rate of 10 °C/min. High temperature Raman spectra were measured by using a Raman spectrometer (LabRAM HR800, HORIBA Jobin Yvon, France). The sintered samples were machined into pellet samples with a thickness of 0.4 mm and a diameter of 8 mm. Then, gold was sputtered on both sides of the pellet samples as the electrodes with a diameter of 6 mm for the dielectric measurements. Temperature dependence of dielectric permittivity and the loss were measured at frequencies of 100 Hz, 1 kHz, 10 kHz, 100 kHz and 1 MHz, by using a LCR meter (4980, Agilent) with a self-made high temperature system. Dielectric properties at microwave frequency were measured with the $TE_{01\delta}$ dielectric resonator method with a network analyzer (HP 8720 Network Analyzer, Hewlett-Packard) and a temperature chamber (Delta 9023, Delta Design, Poway, CA). Room temperature infrared reflectivity spectra were measured by using a Bruker IFS 66v FTIR spectrometer on Infrared beamline station (U4) at National Synchrotron Radiation Lab. (NSRL), China. Dielectric behaviors at terahertz frequencies from 0.2 to 1.2 THz (6.7 - 40 cm^{-1}) were measured by using a terahertz

time-domain (THz TDS) spectroscopy (ADVAVTEST TAS7500SP, Japan). A passive mode-lock fiber laser was used to pump and gate respectively two GaAs photoconductive antennas for the generation and detection of THz wave.

III Results and Discussion

Figure 1 (a) presents *in-situ* XRD patterns of the $Bi_{0.783}(Mo_{0.65}V_{0.35})O_4$ sample over 25 ^{o}C ~ 380 ^{o}C. As discussed in our previous work, the $Bi_{0.783}(Mo_{0.65}V_{0.35})O_4$ sample crystallized in a ordered scheelite-related structure, in which the vacancy and Bi^{3+} cations arranged in an ordered manner. It can be seen that when the temperature was increased to 160 ^{o}C, splitting of the diffraction peaks at 24.07 ^{o}, 39.21 ^{o}, 42.32 ^{o}, and 47.91 ^{o} could be observed, which means that a phase transition took place in the $Bi_{0.783}(Mo_{0.65}V_{0.35})O_4$ sample at this temperature. Besides the peak splitting, several types of abrupt changes were also observed at about 160 ^{o}C, as shown in Fig. 1 (b). With increasing temperature, most diffraction angles decreased linearly in the temperature ranges of below 160 ^{o}C and above 160 ^{o}C, which means that the $Bi_{0.783}(Mo_{0.65}V_{0.35})O_4$ sample possesses a positive temperature expansion coefficient. Many XRD peaks abruptly shifted to the lower angle at the phase transition temperature, which is an evidence of the increase in interplanar spacing. However, in the present situation, due to the phase transition it can not be concluded as usual. The abnormal change trend of the diffraction peaks is a strong evidence of phase transition. Anyway, it is still very difficult to explain exactly how the crystal structure changes during the phase transition, which needs further study.

Thermal expansion curves of the $Bi_{0.783}(Mo_{0.65}V_{0.35})O_4$ and $Bi_{0.883}(Mo_{0.35}V_{0.65})O_4$ ceramics over 25 ~ 400 ^{o}C are presented in Fig. 2. As reported in our previous work,[9] the $Bi_{0.883}(Mo_{0.35}V_{0.65})O_4$ sample crystallized in standard tetragonal scheelite structure.

There is no evidence for any phase transition in the temperature range of 25 ~ 400 $^{\circ}$C and its thermal expansion is linear, as shown in Fig. 2. For $Bi_{0.783}(Mo_{0.65}V_{0.35})O_4$, an abnormality in the thermal expansion curve, i.e. a sudden decrease in the length, was observed at about 150 $^{\circ}$C, which agreed well with the phase transition discussed above. It can be deduced that during the phase transition the crystal cell volume decreased suddenly. Either below or above the phase transition temperature, the $Bi_{0.783}(Mo_{0.65}V_{0.35})O_4$ ceramic possesses positive thermal expansion coefficients + 8 ppm/$^{\circ}$C and + 13.7 ppm/$^{\circ}$C, respectively. This result is in a good agreement with the XRD result.

In-situ Raman spectra and Raman shift of the $Bi_{0.783}(Mo_{0.65}V_{0.35})O_4$ sample as a function of temperature (27 $^{\circ}$C ~ 240 $^{\circ}$C) are shown in Fig. 3. The two strongest modes at 819 cm^{-1} and 887 cm^{-1} belong to the stretching of v_s(V-O) and v_s(Mo-O), respectively. The modes between 200 ~ 700 cm^{-1} were assigned to the bending of δ_s(VO$_4$) and δ_s(Mo-O). The external modes appear at frequencies below 200 cm^{-1}.[9,10] Abrupt changes in the vibration modes could be observed. The external mode at about 98 cm^{-1} slightly red-shifted to 92 cm^{-1} as the temperature was increased from room temperature to 130 $^{\circ}$C and then sharply dropped to about 80 cm^{-1} at 150 $^{\circ}$C. Similar change could also be observed for the strongest band at 819 cm^{-1}. In particular, the bending mode at 600 cm^{-1} disappeared suddenly. All the abnormal changes in the vibration modes resulted from the crystal structural change at 150 $^{\circ}$C.

Dielectric permittivity and dielectric loss of the $Bi_{0.783}(Mo_{0.65}V_{0.35})O_4$ ceramic, as a function of temperature over 30 ~ 350 $^{\circ}$C, at frequencies 100 Hz, 1 kHz, 10 kHz, 100 kHz, 1 MHz, and 7.5 GHz, are shown in Fig. 4. At low frequencies, both dielectric permittivity and dielectric loss increased slowly with temperature when temperature was below 130 $^{\circ}$C and then abruptly increased when temperature reached 150 $^{\circ}$C.

When the frequency was increased to microwave region (about 7.5 GHz), the dielectric permittivity decreased to about 31 at room temperature, while the dielectric loss decreased to about 1×10^{-3}. Due to the temperature limitation (the up-limit is about 150 $^{\circ}$C) of our measurement system for microwave dielectric properties, there was only a trace of abnormal increase in permittivity observed, which corresponded well with the data at low frequency. Meanwhile, the dielectric loss ($\sim1/Q$) increased sharply when temperature was near 150 $^{\circ}$C. Considering the C-M relation ($\varepsilon_x=(3V+8\pi\alpha)/(3V-4\pi\alpha)$, where V is the cell volume and α is the polarizability) and Shannon's additive rule[11] at microwave region, dielectric permittivity is usually determined by the cell volume and polarization (sum of ionic and electronic displacive polarization). Hence, combined with the thermal expansion data shown in Fig. 2, the increase in permittivity should be attributed to the decrease in cell volume.

To further study the intrinsic microwave dielectric properties, the IR reflectivity spectra of the $Bi_{0.783}(Mo_{0.65}V_{0.35})O_4$ ceramic was analyzed using a classical harmonic oscillator model as follows:

$$\varepsilon^*(\omega) = \varepsilon_\infty + \sum_{j=1}^{n} \frac{\omega_{pj}^2}{\omega_{oj}^2 - \omega^2 - j\gamma_j\omega} \tag{1}$$

where $\varepsilon^*(\omega)$ is complex dielectric function, ε_∞ is the dielectric constant caused by the electronic polarization at high frequencies; γ_j, ω_{oj}, and ω_{pj} are the damping factor, the transverse frequency, and plasma frequency of the j-th Lorentz oscillator, respectively, and n is the number of transverse phonon modes. The complex reflectivity $R(\omega)$ can be written as:

$$R(\omega) = \left| \frac{1-\sqrt{\varepsilon^*(\omega)}}{1+\sqrt{\varepsilon^*(\omega)}} \right|^2 \tag{2}$$

Fitted IR reflectivity values and the complex permittivities are shown in Fig. 5. All

the calculated dielectric permittivity and dielectric loss values are almost equal to the measured ones using $TE_{01\delta}$ method, which implies that majority dielectric contribution at microwave region was attributed to the absorptions of structural phonon oscillation at infrared region and very little contribution was from defect phonon scattering. Phonon parameters obtained from the fitting of the infrared reflectivity spectra of the $Bi_{0.783}(Mo_{0.65}V_{0.35})O_4$ ceramic are listed in Table I. It can be seen that the dielectric polarization contribution from the vibration modes below 150 cm^{-1} is above 67 % of the total value, while the electronic displacive polarization holds about 10 % (optical dielectric constant). Similar to other bismuth-based microwave dielectrics, the vibrational modes of Bi-O stretches mainly contributed to the dielectric polarization. From the Shannon's additive rule,[11] the polarizability of Bi^{3+} is about 6.12 $Å^3$ and much larger than the other ions. This can explain the weak contribution from the bending modes of $\delta(VO_4)$ and $\delta(MoO_4)$ over $200 \sim 700$ cm^{-1}.

IV. Conclusions

An abnormal phase transition was revealed in a narrow region in $xBi_{2/3}MoO_4$-$(1-x)BiVO_4$ ($0.5 \leq x \leq 0.7$) solid solution, as demonstrated by $Bi_{0.783}(Mo_{0.65}V_{0.35})O_4$. Unusual shift in XRD angle, Raman spectra and splitting of peaks were observed at 150 ^oC in $Bi_{0.783}(Mo_{0.65}V_{0.35})O_4$. There was a sudden decrease in volume of the $Bi_{0.783}(Mo_{0.65}V_{0.35})O_4$ ceramic at the phase transition temperature (150 ^oC) and the two phases possessed different thermal expansion coefficients (+ 8 ppm/^oC and + 13.7 ppm/^oC, respectively). Due to the decrease in cell volume, the dielectric permittivity sharply increased at about 150 ^oC in a wide frequency range (100 Hz ~ 7.5 GHz). The dielectric polarization mainly came from the Bi-O stretches.

Acknowledgements

References

1 A. W. Sleight, W. J. Linn, *Ann. N. Y. Acad. Sci.*, 1976, **272**, 22.

2 D. Zhou, W. G. Qu, C. A. Randall, L. X. Pang, H. Wang, X. G. Wu, J. Guo, G. Q. Zhang, L. Shui, Q. P. Wang, H. C. Liu, X. Yao, *Acta Mater.*, 2011, **59**, 1502.

3 S. Tokunaga, H. Kato, H. Kudo, *Chem. Mater.*, 2001,**13**,4624

4 H. Liu, J. Yuan, Z. Jiang, W. F. Shangguan, H. Einaga, Y. Teraoka, *J. Mater. Chem.*, 2011, **21**, 16535.

5 A. Kudo, K. Omori, H. Kato, *J. Am. Chem. Soc.*, 1999, **121**, 11459.

6 L. H. Brixner, A. W. Sleight, M. S. Licis, *J. Solid State Chem.*, 1972, **5**, 247.

7 W. Jeitschko, *Acta Crystallogr., Sect. B: Struct. Crystallogr. Cryst. Chem.*, 1973, **29**, 2074.

8 A. W. Sleight, K. Aykan, D. B. Rogers, *J. Solid State Chem.*, 1975, **13**, 231.

9 D. Zhou, W. B. Li, L. X. Pang, J. Guo, Z. M. Qi, T. Shao, X. Yao, C. A. Randall, *Dalton Trans.*, 2014, **43**, 7290.

10 N. Weinstoc, H. Schulze, A. Muller, *J. Chem. Phys.*, 1973, **59**, 5063

11 R.D. Shannon, *J. Appl. Phys.*, 1993, **73**, 348.

Table I. Phonon parameters obtained from the fitting of the infrared reflectivity

spectra of $Bi_{0.783}(Mo_{0.65}V_{0.35})O_4$ ceramic

Mode	ω_{oj}	ω_{pj}	γ_j	$\Delta\varepsilon_j$
1	68.09	190.10	22.33	7.80
2	90.30	299.20	30.11	11.00
3	116.93	290.57	38.50	6.17
4	158.44	107.12	32.33	0.46
5	198.12	105.51	36.56	0.28
6	254.29	150.31	41.94	0.35
7	290.91	184.45	32.09	0.40
8	325.87	220.85	41.79	0.46
9	377.98	256.77	59.20	0.46
10	429.47	332.5	68.58	0.60
11	536.43	340.19	93.87	0.40
12	590.77	283.24	81.84	0.98
13	706.29	421.18	69.11	0.36
14	776.75	263.28	60.17	0.12
15	826.22	293.96	52.15	0.13
16	899.65	98.00	32.06	0.01
	ε_∞=3.61		ε_0=33.58	

Figure Captions:

Fig. 1 *in-situ* X-ray diffraction patterns of the $Bi_{0.783}(Mo_{0.65}V_{0.35})O_4$ sample (a) and selected characteristic diffraction angles as a function of temperature (b) (25 ^{o}C ~ 380 ^{o}C)

Fig. 2 Thermal expansion curves of the $Bi_{0.783}(Mo_{0.65}V_{0.35})O_4$ and $Bi_{0.883}(Mo_{0.35}V_{0.65})O_4$ ceramics in the temperature range 25 ~ 400 ^{o}C

Fig. 3 *In-situ* Raman spectra (a) and Raman shift (b) of the $Bi_{0.783}(Mo_{0.65}V_{0.35})O_4$ sample as a function of temperature range (27 ^{o}C ~ 240 ^{o}C)

Fig. 4 Dielectric permittivity (a) and dielectric loss (b) of the $Bi_{0.783}(Mo_{0.65}V_{0.35})O_4$ ceramic as a function of temperature in the range 30 ~ 350 ^{o}C at frequencies 100 Hz, 1 kHz, 10 kHz, 100 kHz, 1 MHz, and 7.5 GHz

Fig. 5 Measured and calculated infrared reflectivity spectra (solid line for fitting values and circle for measured values)[9] and complex dielectric spectra of the $Bi_{0.783}(Mo_{0.65}V_{0.35})O_4$ ceramic (circles are experimental at microwave region and THz data, solid lines represent the fit of IR spectra)
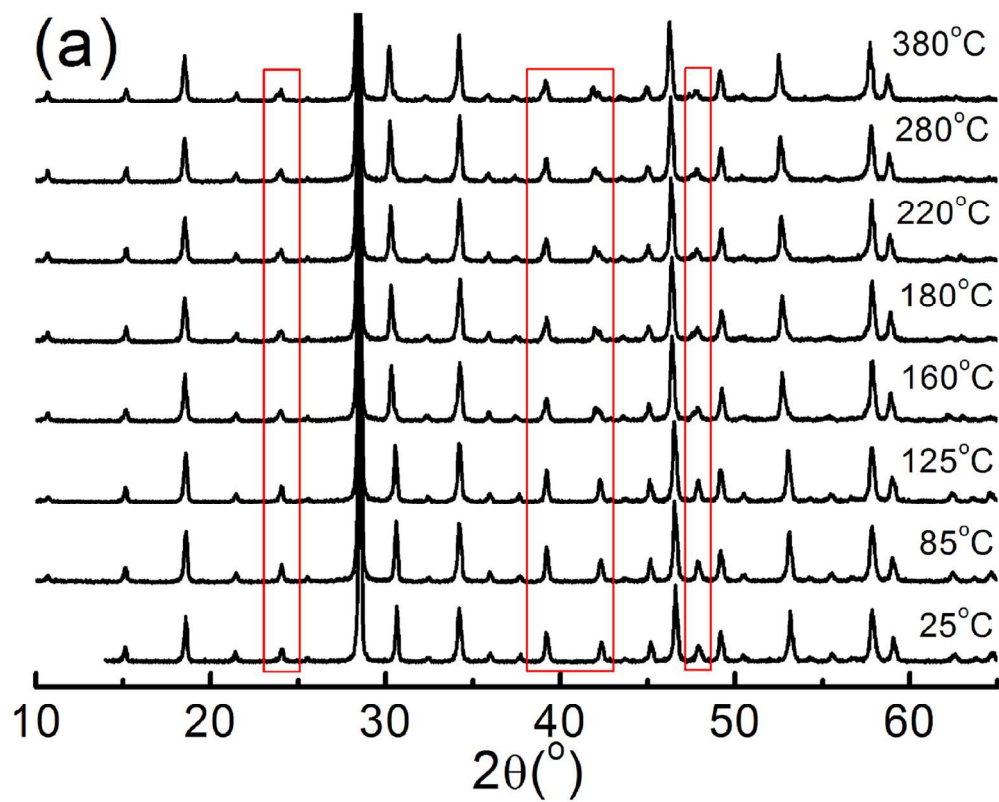
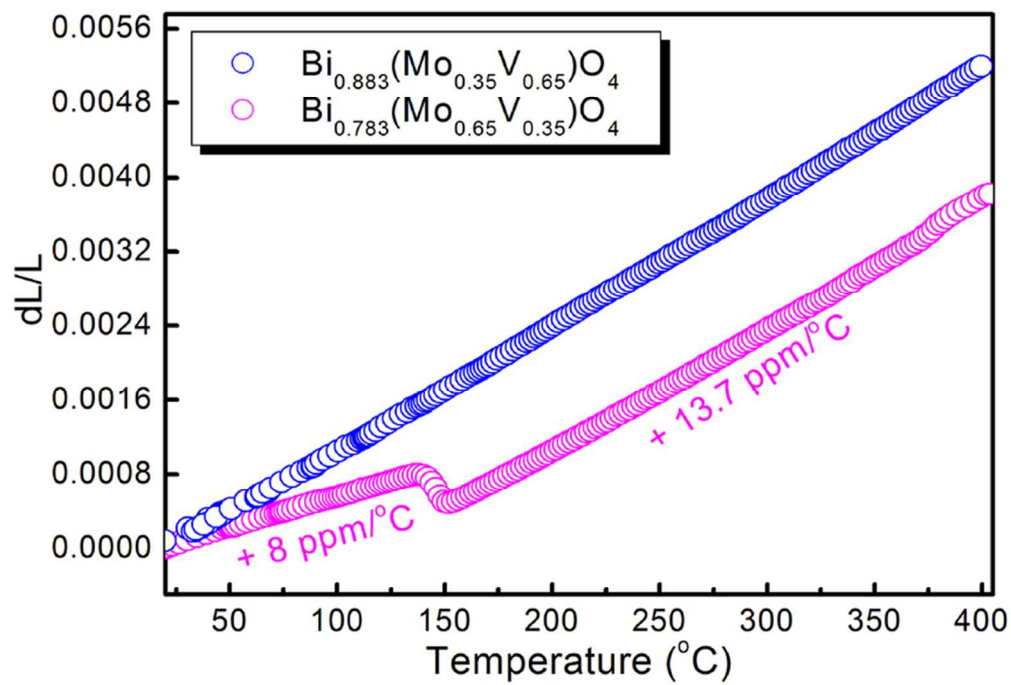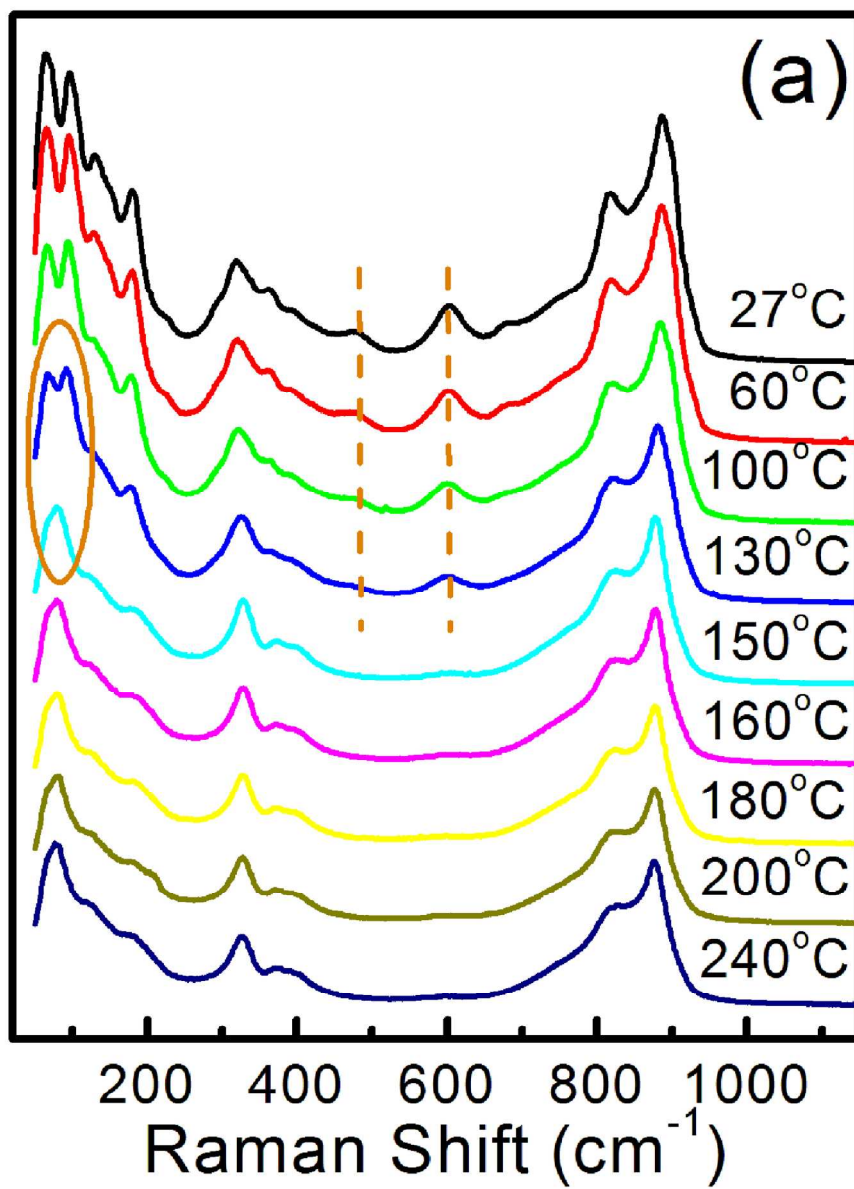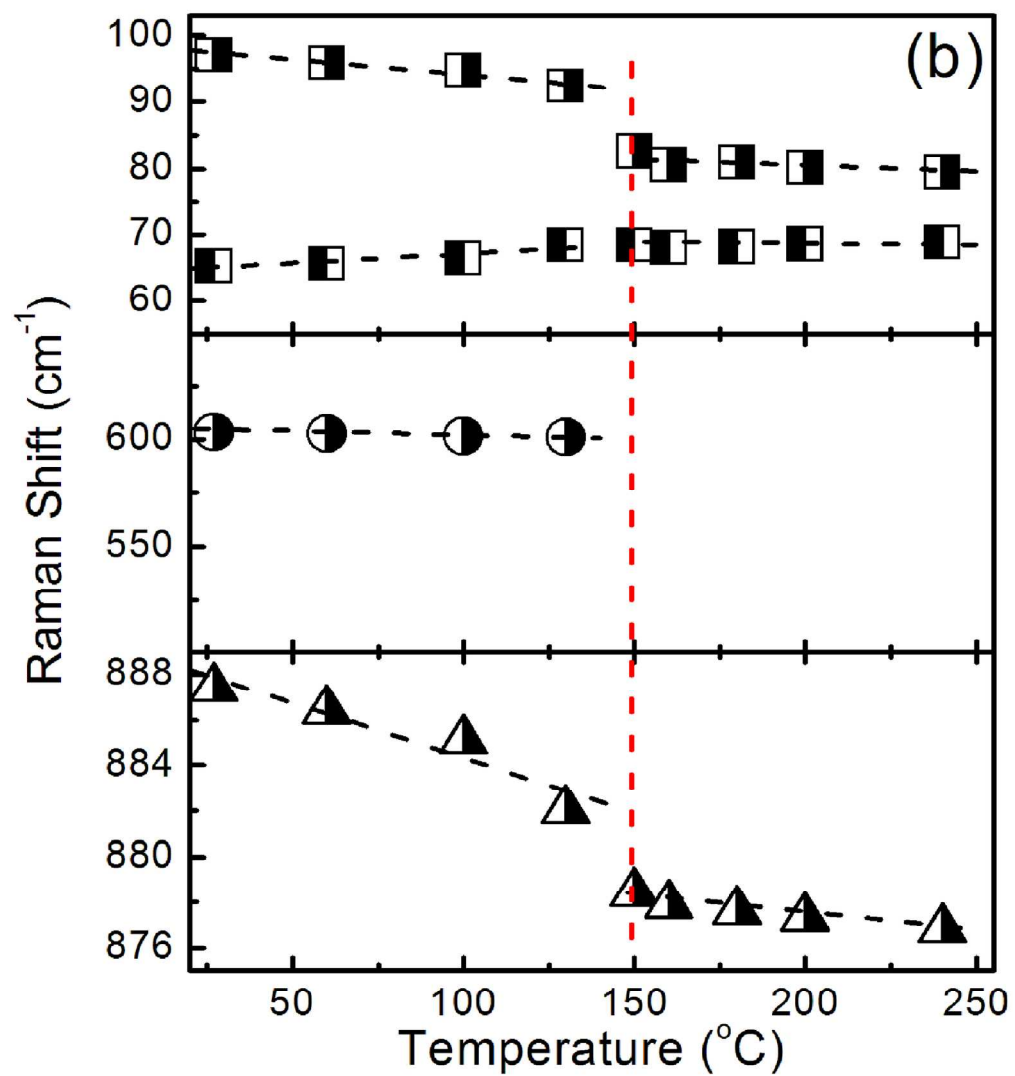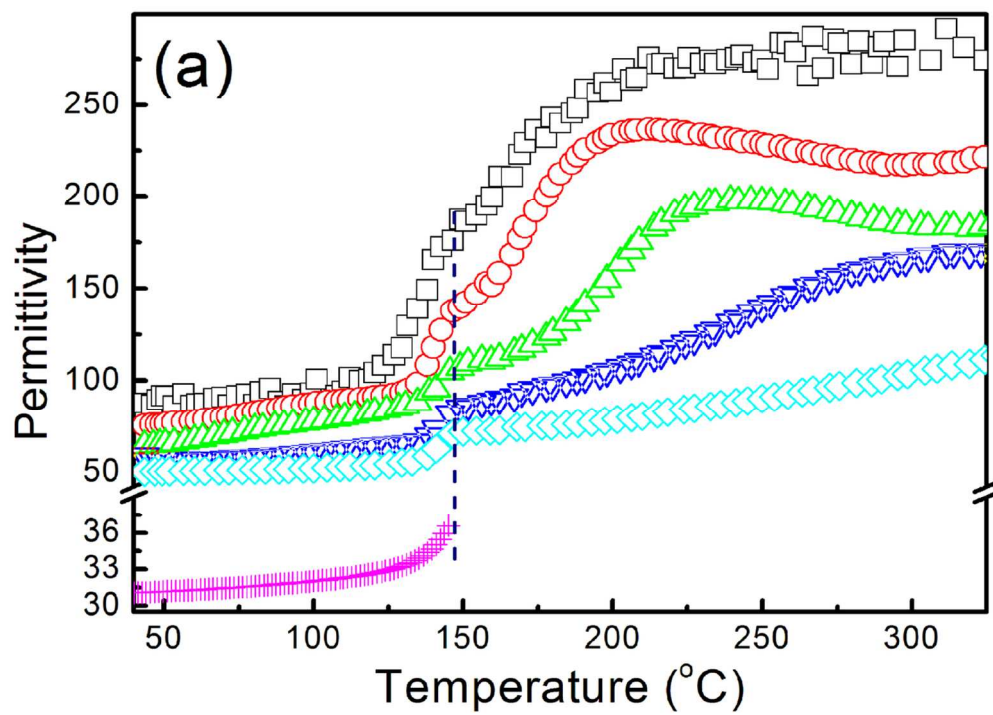63x50mm (600 x 600 DPI)
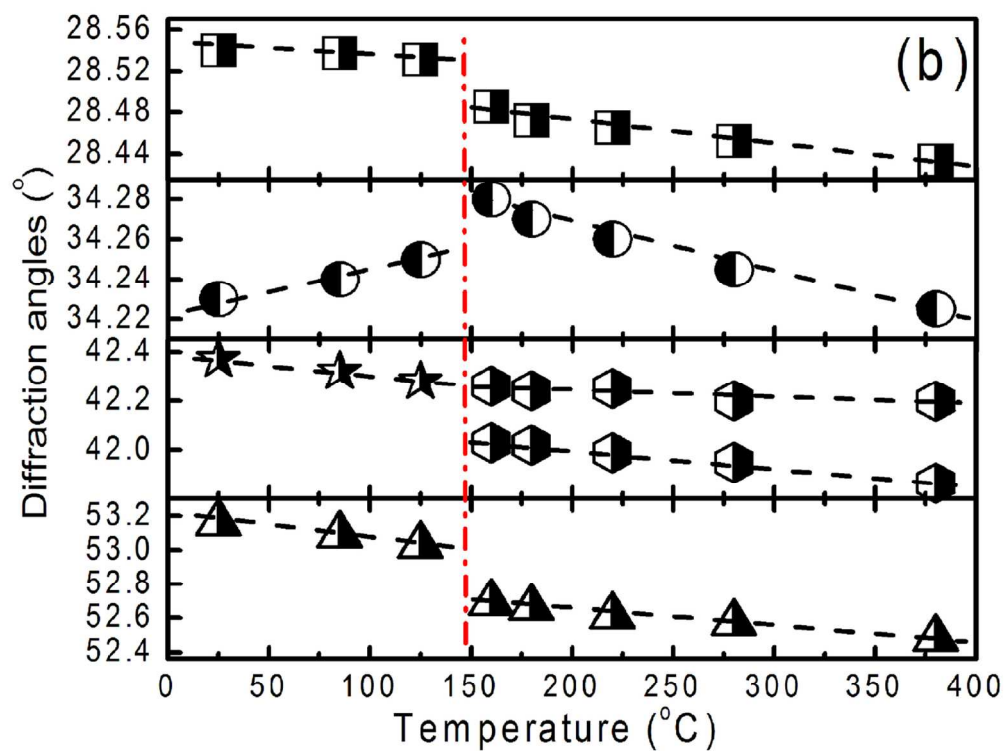
63x50mm (600 x 600 DPI)

Fig. 2 Thermal expansion curves of the Bi0.783(Mo0.65V0.35)O4 and Bi0.883(Mo0.35V0.65)O4 ceramics in the temperature range 25 ~ 400 oC
72x49mm (300 x 300 DPI)

95x114mm (600 x 600 DPI)
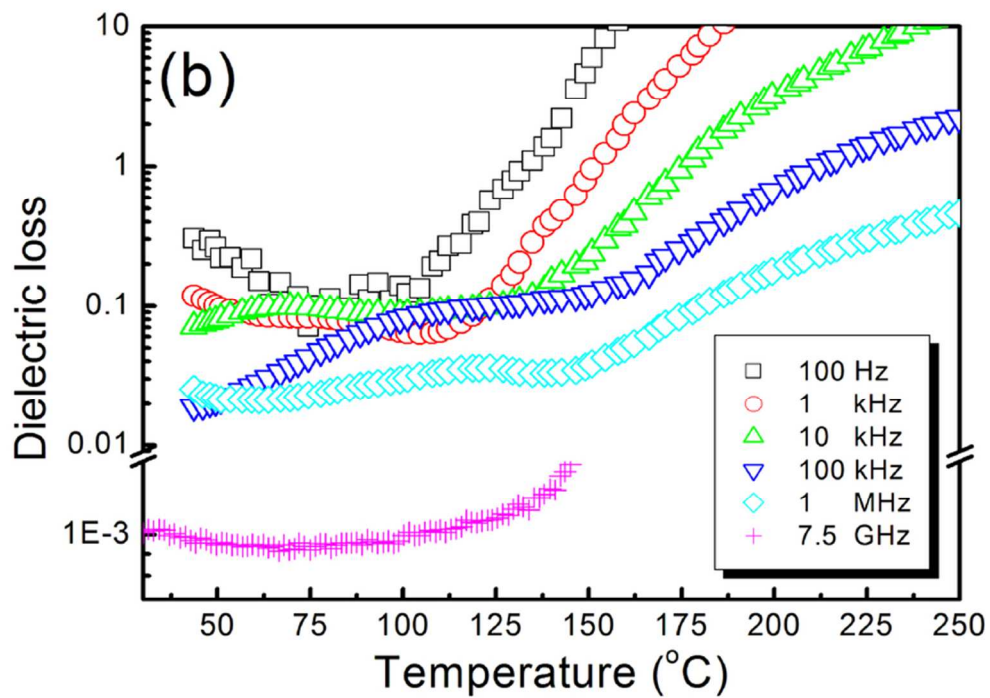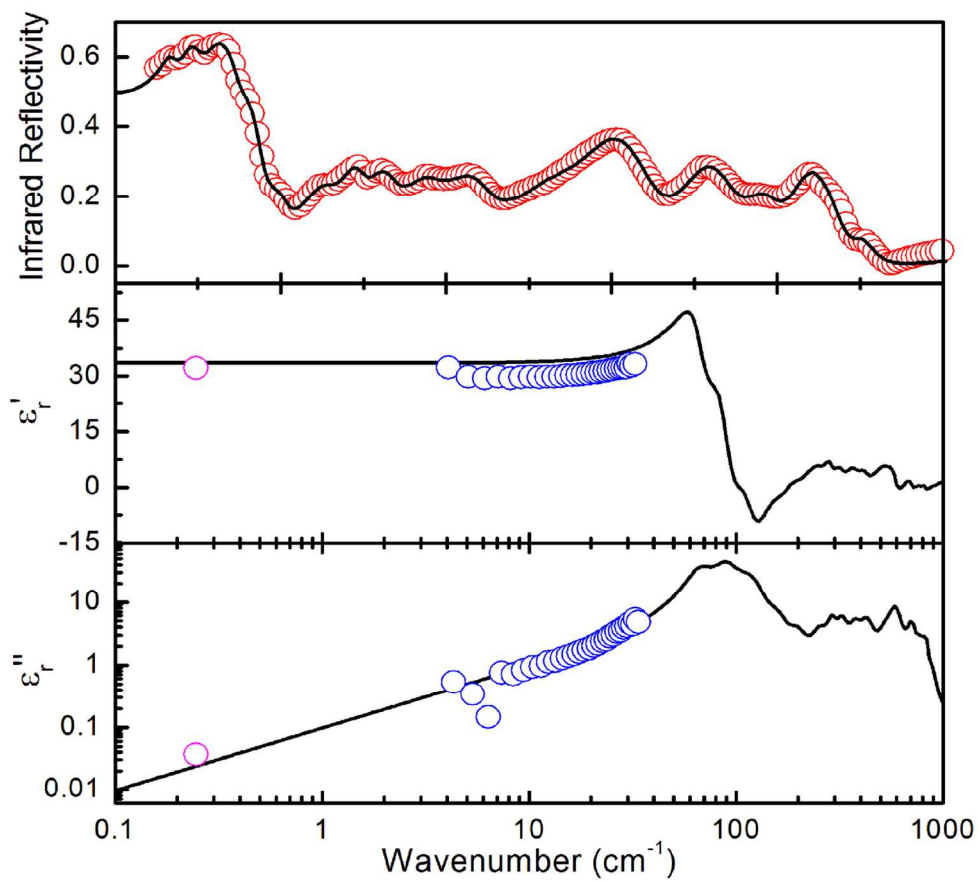
87x96mm (600 x 600 DPI)

58x42mm (600 x 600 DPI)

Fig. 4 Dielectric permittivity (a) and dielectric loss (b) of the Bi0.783(Mo0.65V0.35)O4 ceramic as a function of temperature in the range 30 ~ 350 oC at frequencies 100 Hz, 1 kHz, 10 kHz, 100 kHz, 1 MHz, and 7.5 GHz
73x51mm (300 x 300 DPI)

70x62mm (600 x 600 DPI)